http://dx.doi.org/10.5012/bkcs.2014.35.5.1465

Studies on Ionic Conduction in $Ce_{0.95}Eu_{0.05}P_2O_7$ at Intermediate Temperatures

Hongtao Wang,* Lin Sun, Chunhua Luo, and Suhua Fan

College of Chemistry and Chemical Engineering, Fuyang Teachers College, Fuyang 236041, China
**E-mail: hongtaoking3@126.com*
Received December 16, 2013, Accepted January 23, 2014

In this study, an intermediate temperature ionic conductor, $Ce_{0.95}Eu_{0.05}P_2O_7$, was prepared by solid state reaction. The variation of conductivities with the pressure pH_2O or time were studied. The highest conductivity of $Ce_{0.95}Eu_{0.05}P_2O_7$ sample was observed in dry air atmosphere at 300 °C to be 1.1×10^{-4} S·cm^{-1} and in wet air atmosphere ($pH_2O = 7.4 \times 10^3$ Pa) at 100 °C to be 1.4×10^{-3} S·cm^{-1}, respectively. The log σ ~ log (pO_2) plot result indicated that $Ce_{0.95}Eu_{0.05}P_2O_7$ was almost a pure ionic conductor under high oxygen partial pressure and a mixed conductor of ion and electron under low oxygen partial pressure.

Key Words : Cerium pyrophosphate, XRD, Conductivity, Electrolyte

Introduction

Fuel cells operated at intermediate temperatures (100-600 °C) have been paid much attention since they can increase the operating life of the cells and decrease the risk of delamination of the cell components.[1-4] For operation at intermediate temperature, two routes have been adopted. One is to develop the electrolyte membrane. The other more effective route is to search new electrolytes with higher ionic conductivities at intermediate temperature.

Pyrophosphate salts were known to exhibit high protonic conductivities in the 100-400 °C temperature range.[5-9] Hibino and co-workers have demonstrated that Al^{3+}, In^{3+} and Mg^{2+} doped SnP_2O_7 have high protonic conductivities of above 10^{-2} S·cm^{-1} under unhumidified conditions in this temperature range.[10,11] Ma *et al.* reported that the highest conductivities were observed for the sample of $Sn_{0.91}Ga_{0.09}P_2O_7$ to be 4.6×10^{-2} S·cm^{-1} at 175 °C[12] and $Sn_{0.94}Sc_{0.06}P_2O_7$ to be 2.8×10^{-2} S·cm^{-1} at 200 °C[13] in wet H_2, respectively. Wang *et al.*[14] and Tsai *et al.*[15] reported the conductivities of CeP_2O_7 kept above 10^{-2} S·cm^{-1} under moist conditions in the intermediate temperature range.

However, the ionic conduction of the reported CeP_2O_7-based materials were yet not too clear. The effective ionic radius of Eu^{3+} is 0.095 nm, which is close to that of Ce^{4+} (0.087 nm) in 6-fold coordination.[16] Therefore, it is interesting to investigate the CeP_2O_7 with Eu^{3+} as dopant. In this paper, $Ce_{0.95}Eu_{0.05}P_2O_7$ was prepared by solid state reaction. The structural characteristics of the sample was analyzed using XRD and SEM. Electrochemical properties were also investigated using some electrochemical methods at intermediate temperatures (100-300 °C).

Experimental

The initial molar ratios of phosphorus vs. metal ions, P_{ini}/(Ce + Eu), should be controlled to be 2.3 due to a fraction of phosphorus loss in the process by vaporization.[6,12] The $Ce_{0.95}Eu_{0.05}P_2O_7$ was synthesized via the conventional solid-state reaction method. The required amounts of CeO_2, Eu_2O_3 (99.99%) and 85% H_3PO_4 reagents were fully mixed for 0.5 h with an alumina crucible and then held at 300 °C while stirring from slurry to a dry paste until a solid mixture was formed. In order to promote the following reaction[7] $CeO_2 + 2H_3PO_4 = CeP_2O_7 + 3H_2O \uparrow$ carried on, the resulting mixture heat-treated at 350 °C for 1 h until it became yellowish powder. The calcined powder was reground and uniaxially pressed into pellet (diameter 20 mm, thickness 2 mm) under 120 MPa. The pellet annealed at 350 °C for 4 h in a muffle furnace to yield the desired sample. The phase structure of the $Ce_{0.95}Eu_{0.05}P_2O_7$ was detected by the X–ray diffraction (XRD) with a Panalytical X′ Pert Pro MPD diffractometer. The microscopic feature of the $Ce_{0.95}Eu_{0.05}P_2O_7$ was performed by a scanning electron microscope (SEM).

For the electrochemical determinations, round plate roughly 19.3 mm in diameter with a thickness of about 1.0 mm was produced. 20%Pd-80%Ag paste was smeared on both sides (area: 0.5 cm^2) of the sample which acted as electrodes. The impedance spectra were recorded over the frequency range from 0.1 Hz to 1 MHz with an electrochemical analyzer (CHI660E made in China). The conductivity measurements in dry and wet air atmospheres as a function of temperature or time were performed. For comparison, the CeP_2O_7 sample was also prepared. The conductivity as the function of oxygen partial pressure (pO_2) was measured in the pO_2 range of 1-10^{-20} atm. The pO_2 was accommodated by commixing O_2, air, N_2, H_2O and H_2 in proper ratio, and measured using an oxygen sensor on line.

Results and Discussion

Structure of the Sample. For the ideal cubic structure, the tolerance factor *t* should equal one. The more *t* deviates from unity, the less stable the cubic structure. The incorporation of Eu into the CeP_2O_7 lattice was conducted systematically because the large ionic radius of trivalent Eu is 0.095 nm,

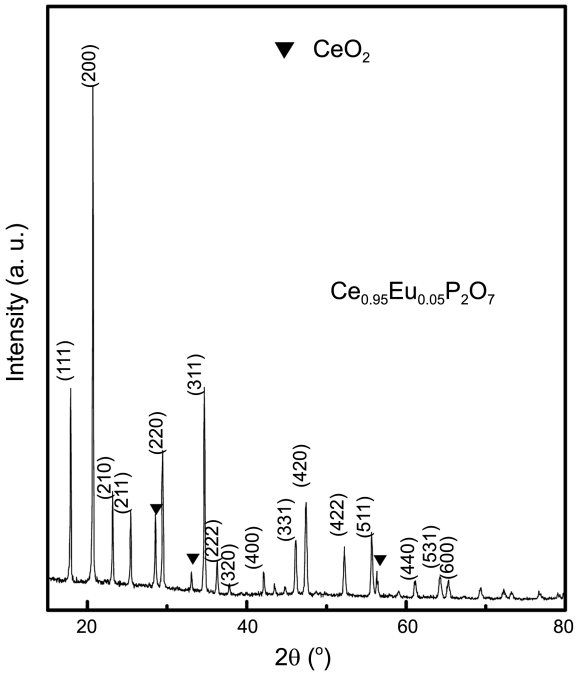

Figure 1. XRD pattern of the $Ce_{0.95}Eu_{0.05}P_2O_7$ sample.

which is close to that of Ce^{4+} (0.087 nm) in 6-fold coordination.[16] Figure 1 showed XRD pattern at room temperature of the $Ce_{0.95}Eu_{0.05}P_2O_7$ sample. The XRD angles at 17.93º, 20.77º, 23.24º, 25.48º, 29.49º, 34.74º, 36.34º, 37.88º, 42.19º, 46.20º, 47.48º, 52.36º, 55.79º, 61.24º, 64.36º and 65.37º belonged to the (111), (200), (210), (211), (220), (311), (222), (320), (400), (331), (420), (422), (511), (440), (531) and (600) crystal planes of CeP_2O_7, respectively.[15] As shown, the $Ce_{0.95}Eu_{0.05}P_2O_7$ was in agreement with the cubic phase structure of CeP_2O_7 in JCPDS 16-0584. Besides, there were some additional peaks of CeO_2 impurity, although the initial P_{ini}/(Ce + Eu) molar ratio was kept at 2.3 to avoid the impurity of CeO_2. The sample sintered at 350 °C in order to minimize the surface-adsorbed or intergranular water species during the conductivity measurements.[6]

SEM Image. Typical SEM image of the cross section of the $Ce_{0.95}Eu_{0.05}P_2O_7$ heat-treated at 350 °C for 4 h was displayed in Figure 2. From the SEM image, the sample exhibited a fine uniform microstructure, though there were some pores occur in sample. The relative density of the $Ce_{0.95}Eu_{0.05}P_2O_7$ sample prepared in this study was estimated to be ~82.4%, somewhat lower than those reported for Sr^{2+} and Mg^{2+}-doped CeP_2O_7 prepared through similar heat treatments.[6,15]

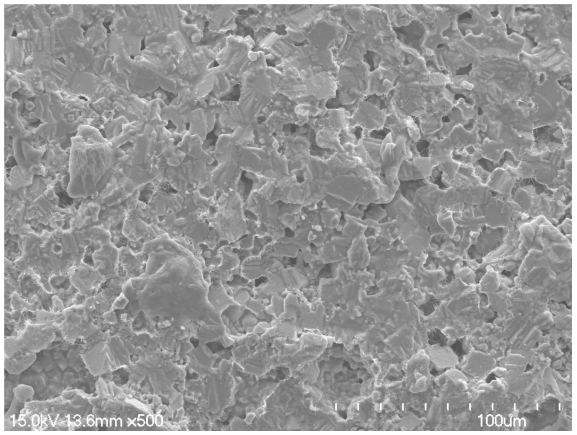

Figure 2. The cross-sectional SEM image of the $Ce_{0.95}Eu_{0.05}P_2O_7$ sample.

Ionic Conductivities in Dry and Wet Air Atmospheres. Figure 3 showed temperature dependence of the conductivities of the $Ce_{0.95}Eu_{0.05}P_2O_7$ and CeP_2O_7 samples in dry air atmosphere at 100-300 ºC. As can be seen from Figure 3, one to two orders conductivities of undoped CeP_2O_7 lower than that of 5 mol % Eu^{3+} doped CeP_2O_7. This may be explained by the reason described previously in Ref..[13] Ma *et al.*[13] reported that the higher Sc^{3+} doping level resulted in the higher oxygen vacancy concentration and the effective concentration of oxygen vacancy may reach its maximum value in $Sn_{0.94}Sc_{0.06}P_2O_7$ sample. It is clear that the conductivities of the Sc^{3+} doped samples are higher than the conductivities of undoped SnP_2O_7.[13] Therefore, the higher conductivities of the $Ce_{0.95}Eu_{0.05}P_2O_7$ are resulted from the substitution of Eu^{3+} for Ce^{4+}-site which increased the concentration of mobile charge carriers. The highest conductivities were observed for the $Ce_{0.95}Eu_{0.05}P_2O_7$ and CeP_2O_7 to be 1.1×10^{-4} $S \cdot cm^{-1}$ and 4.2×10^{-6} $S \cdot cm^{-1}$ at 300 ºC, respectively. However, the conductivities of $Ce_{0.95}Eu_{0.05}P_2O_7$ were much lower than the reported values of CeP_2O_7 (~10^{-2} $S \cdot cm^{-1}$).[14,15] It can be related to large difference in particle size and morphology of SEM image and the synthetic history.[17]

Figure 4 showed the variation of conductivities of $Ce_{0.95}Eu_{0.05}P_2O_7$ and CeP_2O_7 with time during humidification

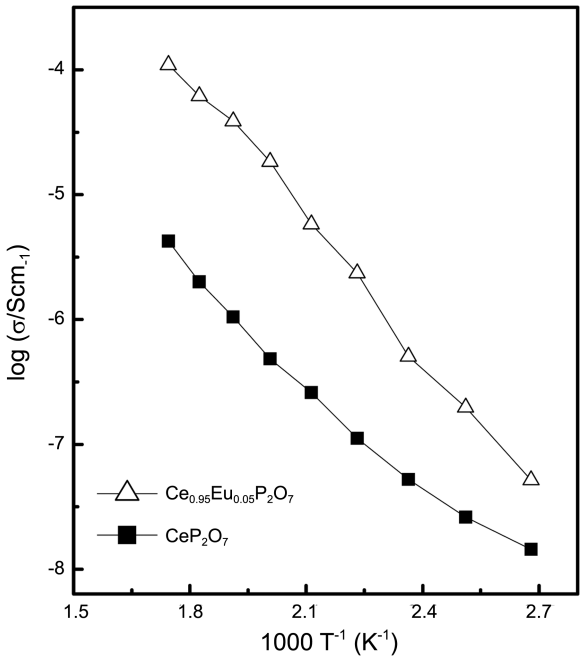

Figure 3. Temperature dependence of conductivities of the $Ce_{0.95}Eu_{0.05}P_2O_7$ and CeP_2O_7 samples in dry air atmosphere at 100-300 ºC.

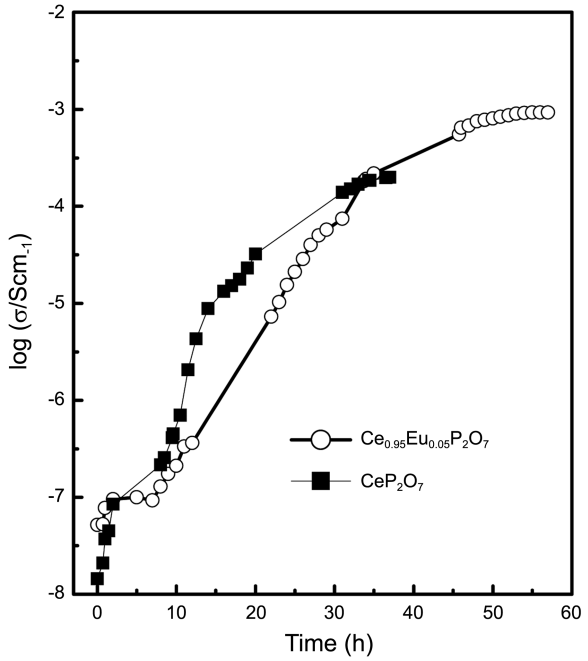

Figure 4. The variation of conductivities of $Ce_{0.95}Eu_{0.05}P_2O_7$ and CeP_2O_7 samples with time during humidification in air at 100 °C ($pH_2O = 3.2 \times 10^3$ Pa).

in air at 100 °C ($pH_2O = 3.2 \times 10^3$ Pa). The humidification was a slow process. For the interpretation of our data, we consider the introduction of hydroxyd ion $OH_o^{\bullet}$ into the samples by the following two reactions. Therefore, the contribution of hole conduction decreased and proton conduction appeared.

$$H_2O(g) + V_o^{\bullet\bullet} + O_o^{\times} \Leftrightarrow 2OH_o^{\bullet} \quad (1)$$

$$H_2O(g) + 2h^{\bullet} + 2O_o^{\times} \Leftrightarrow 2OH_o^{\bullet} + 1/2O_2 \quad (2)$$

As can be seen from Figure 4, there was about four orders of magnitude increased in conductivities and higher conductivity level could be achieved after about 50 h to reach a steady state. From this recovery it is concluded that the humidification process not only led to the formation of $OH_o^{\bullet}$ in the samples, as expressed by Eqs. (1) and (2), but also introduced some water species (H_2O or H_3O^+) into the samples, which can act as charge carriers and increase in conductivities.[6]

Figure 5 showed the variation of conductivities of the $Ce_{0.95}Eu_{0.05}P_2O_7$ sample with time while the pH_2O pressure changing from 3.2×10^3 Pa to 7.4×10^3 Pa in air at 100 °C. Correspondingly, the conductivities were observed from 9.3×10^{-4} S·cm^{-1} to 1.4×10^{-3} S·cm^{-1} with saturating water vapor increased. The observation can be explained using Eqs. (1) and (2). The increasing pH_2O pressure shifted the Eqs. (1) and (2) toward the right side, resulting in an increase of the proton concentration in the $Ce_{0.95}Eu_{0.05}P_2O_7$ sample.

In order to investigate the ionic conductivities of the $Ce_{0.95}Eu_{0.05}P_2O_7$ sample, the relationship between the conductivities and the oxygen partial pressure ($pO_2 = 10^{-20} \sim 1$ atm) was measured. Figure 6 showed the plot of log $\sigma \sim$ log

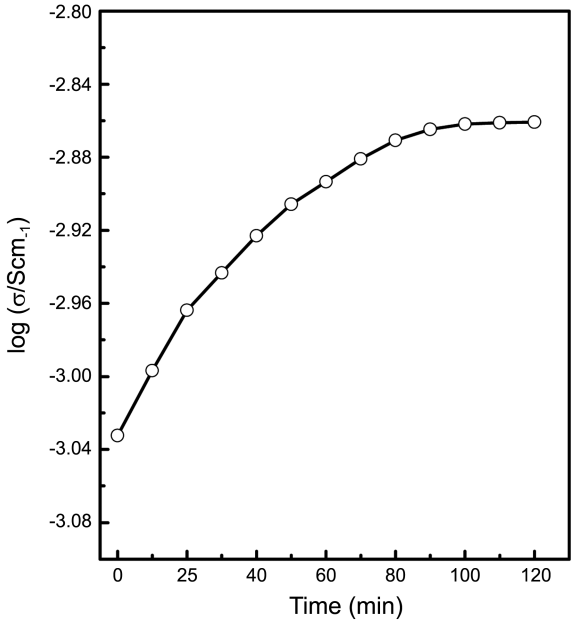

Figure 5. Time dependence of conductivities of the $Ce_{0.95}Eu_{0.05}P_2O_7$ sample while the pH_2O pressure changing from 3.2×10^3 Pa to 7.4×10^3 Pa in air at 100 °C.

(pO_2) in wet air atmosphere ($pH_2O = 3.2 \times 10^3$ Pa) at 100 °C. It is clear that the conductivities were almost independent of pO_2, confirming that $Ce_{0.95}Eu_{0.05}P_2O_7$ was almost a pure ionic conductor at high oxygen partial pressure range. While in hydrogen-containing atmosphere, the protonic conduction becomes dominant as can be seen from Eq. (3). The total conductivities increased with the decreasing oxygen partial pressure indicated that it is a mixed conductor of ion and electron in hydrogen-containing atmosphere. This may

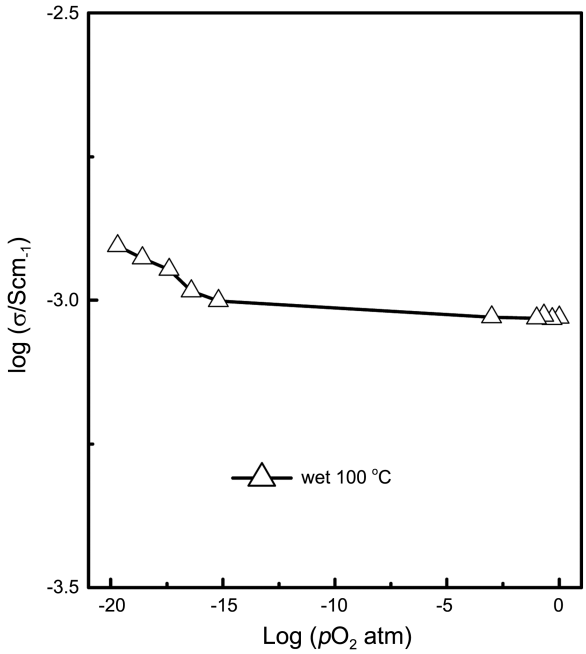

Figure 6. The conductivities of the $Ce_{0.95}Eu_{0.05}P_2O_7$ sample as a function of pO_2 in air ($pH_2O = 3.2 \times 10^3$ Pa) at 100 °C.

be due to the reduction of Ce^{4+} to Ce^{3+} to a certain extent at low oxygen partial pressure range. In conclusion, $Ce_{0.95}Eu_{0.05}P_2O_7$ is a good intermediate temperature solid ion conductor although its conductivity is low. It has been reported that excess H_3PO_4 or P_mO_n layer can increase the sample conductivity by providing additional pathways for proton transport.[10,18] Therefore, it could apply CeP_2O_7-based material as electrolyte to the fuel cells by forming composite electrolyte.[18]

$$H_2 + 2O_o^{\times} \Leftrightarrow 2OH_o^{\bullet} + 2e' \quad (3)$$

Conclusion

In this paper, an intermediate temperature ionic conductor, $Ce_{0.95}Eu_{0.05}P_2O_7$, was prepared. The XRD result confirmed that the $Ce_{0.95}Eu_{0.05}P_2O_7$ exhibited cubic phase structure of cerium pyrophosphate. The variation of conductivities with time during humidification process revealed the humidification was a slow process and there was about four orders of magnitude increased in conductivities. The conductivities of $Ce_{0.95}Eu_{0.05}P_2O_7$ increased from 9.3×10^{-4} S·cm^{-1} to 1.4×10^{-3} S·cm^{-1} while the pH_2O pressure changing from 3.2×10^3 Pa to 7.4×10^3 Pa in air at 100 °C. The log $\sigma \sim$ log (pO_2) plot result indicated that $Ce_{0.95}Eu_{0.05}P_2O_7$ was almost a pure ionic conductor under high oxygen partial pressure and the protonic conduction became dominant under low oxygen partial pressure.

Acknowledgments. This work was supported by the National Natural Science Foundation of China (No. 21201037), the Natural Science Foundation of the Anhui Higher Education Institutions of China (No.KJ2013B193), and the Specialized Research Fund for the Doctoral Program of Fuyang Teachers College 2012.

References

1. Hyun, S. H.; Kim, A. R.; Nahm, K. S.; Yoo, D. J. *Bull. Korean Chem. Soc.* **2012**, *33*, 375.
2. Lee, H-J.; Lee, D. H.; Henkensmeier, D.; Jang, J. H.; Cho, E. A.; Kim, H-J.; Kim, H. *Bull. Korean Chem. Soc.* **2012**, *33*, 3279.
3. Haile, S. M.; Boysen, D. A.; Chisholm, C. R. I.; Merle, R. B. *Nature* **2001**, *410*, 910.
4. Lim, Y. T.; Son, J. Y. *Bull. Korean Chem. Soc.* **2013**, *34*, 9.
5. Shen, Y. B.; Kojima, K.; Nishida, M.; Heo, P.; Choi, K. H.; Chang, H.; Hibino, T. *J. Meter. Chem.* **2012**, *22*, 14907.
6. Singh, B.; Im, H.-N.; Park, J.-Y.; Song, S.-J. *J. Phys. Chem. C* **2013**, *117*, 2653.
7. Sato, Y.; Shen, Y. B.; Nishida, M.; Kanematsu, W.; Hibino, T. *J. Meter. Chem.* **2012**, *22*, 3973.
8. Wang, H.; Sun, L.; Chen, J.; Luo, C. *Acta Phys.-Chim. Sin.* **2012**, *28*, 2893.
9. Shen, Y. B.; Heo, P.; Pak, C.; Chang, H.; Hibino, T. *Electrochem. Commun.* **2012**, *24*, 82.
10. Tomita, A.; Kajiyama, N.; Kamiya, T.; Nagao, M.; Hibino, T. *J. Electrochem. Soc.* **2007**, *154*, B1265.
11. Genzaki, K.; Heo, P.; Sano, M.; Hibino, T. *J. Electrochem. Soc.* **2009**, *156*, B806.
12. Wang, H.; Liu, J.; Wang, W.; Ma, G. *J. Power Sources* **2010**, *195*, 5596.
13. Wang, H.; Zhang, H.; Xiao, G.; Zhang, F.; Yu, T.; Xiao, J.; Ma, G. *J. Power Sources* **2011**, *196*, 683.
14. Sun, X.; Wang, S.; Wang, Z.; Ye, X.; Wen, T.; Huang, F. *Solid State Ionics* **2008**, *179*, 1138.
15. Le, M.-V.; Tsai, D.-S.; Yang, C.-Y.; Chung, W.-H.; Lee, H.-Y. *Electrochim. Acta* **2011**, *56*, 6654.
16. Shannon, R. D. *Acta Cryst.* **1976**, *A32*, 751.
17. Tao, S. *Solid State Ionics* **2009**, *180*, 148.
18. Lan, R.; Xu, X.; Tao, X.; Irvine, J. T. S. *J. Power Sources* **2010**, *195*, 6983.